

## Control and analysis of simple-structured robot arm using flexible pneumatic cylinders



Mohd Aliff<sup>1,\*</sup>, Shujiro Dohta<sup>2</sup>, Tetsuya Akagi<sup>2</sup>

<sup>1</sup>*Instrumentation and Control Engineering, Malaysian Institute of Industrial Technology, Universiti Kuala Lumpur, Persiaran Sinaran Ilmu, 81750 Bandar Seri Alam, Johor Bahru, Johor, Malaysia*

<sup>2</sup>*Department of Intelligent Mechanical Engineering, Okayama University of Science, Okayama, Japan*

### ARTICLE INFO

#### Article history:

Received 20 December 2016

Received in revised form

20 September 2017

Accepted 15 October 2017

#### Keywords:

Pneumatic robot arm

Flexible pneumatic cylinder

Master-slave control

PWM control valve

### ABSTRACT

The flexible pneumatic cylinder is a novel pneumatic actuator that can work even if the cylinder bends. The purpose of this study is to develop a simple-structured rehabilitation device using the flexible pneumatic cylinder. In this paper, the control and analysis of robot arm for the human wrist rehabilitation by using flexible pneumatic cylinder is introduced. The system consists of a slave arm, a master arm, a high-speed microcomputer, compact and inexpensive quasi-servo valves, a potentiometer and accelerometers to give the references for the attitude control. The control performances of the device were also investigated. Then, it is needed to improve the control performance of the devices. Therefore, the analytical model of the flexible pneumatic cylinder and the quasi servo valve with the embedded controller was proposed and tested for estimating the performance theoretically. The comparison between the theoretical and experimental results was also executed to confirm the validity of the proposed model.

© 2017 The Authors. Published by IASE. This is an open access article under the CC BY-NC-ND license (<http://creativecommons.org/licenses/by-nc-nd/4.0/>).

### 1. Introduction

One of the social complications encountered by developed countries is the elderly population is continuously increasing while the birth rates remain to decline. These population differences become more apparent every year and are raising the concerns of professionals from a variety of fields including the social sciences, medicine and engineering. Today, numerous studies have shown that robots can be beneficial and advantageous to healthcare providers in a variety of ways from supporting in nursing care (Ishii et al., 2005; Noritsugu et al., 2009) such as support the activities of daily life for the elderly and the disabled (Kobayashi et al., 2004) until to performing complex surgical procedures (Piquion et al., 2009). The capacity of doing precision work reliably and repetitively for long periods would be of great value in this field. In the middle of the numerous robots designed to deliver arm therapy, ARM-GUIDE (Reinkensmeyer et al., 1999) and MIME (Lum et al., 2004) are two representative devices that have been

verified extensively with patients. ARM-GUIDE that allows the patient to exercise against gravity can be used as diagnostic tool and a treatment tool for addressing arm impairment. However, these robotic arms are heavy in weight and must be fixed on walls and poles. This causes the limited space in motion and patients are easily to feel excess fatigue. Furthermore, these robots are complex to set up by patients themselves and are not appropriate for rehabilitation training program at home (Zheng et al., 2006). The purpose of our study is to develop a flexible and lightweight actuator and to apply it to a flexible robot arm (Yassin et al., 2016) and rehabilitation device. Novel types of the flexible pneumatic actuator that can be used even if the actuators are deformed by the external forces have been proposed and tested (Akagi and Dohta, 2007; Dohta et al., 2013). The flexible robot arm with simple structure has been proposed and tested by using the flexible pneumatic cylinders (Aliff et al., 2012; Aliff et al., 2014). This robot arm has three degrees-of-freedom that is bending, extending and contracting. The master-slave control is adopted into the robot arm as a control method in order to be used in rehabilitation field. The master-slave control is necessary when a physical therapist wants to give a rehabilitation motion to a patient. During rehabilitation, the therapist will control the movement of the robot by holding the master arm

\* Corresponding Author.

Email Address: [mohdaliff@unikl.edu.my](mailto:mohdaliff@unikl.edu.my) (M. Aliff)

<https://doi.org/10.21833/ijaas.2017.012.026>

2313-626X/© 2017 The Authors. Published by IASE.

This is an open access article under the CC BY-NC-ND license

(<http://creativecommons.org/licenses/by-nc-nd/4.0/>)

and move it repeatedly according to conditions and needs of the patient. At the same time, the patient's arm will follow the movement by holding the slave arm as shown in Fig. 1. In this paper, the control and analysis of robot arm for the human wrist rehabilitation by using flexible pneumatic cylinder is introduced. The system consists of a slave arm, a master arm, a high-speed microcomputer, compact and inexpensive quasi-servo valves, a potentiometer and accelerometers to give the references for the attitude control. Then, the analytical model of the flexible pneumatic cylinder and the quasi servo valve with the embedded controller was proposed and tested. The comparison between the theoretical and experimental results was also executed to confirm the validity of the proposed model.

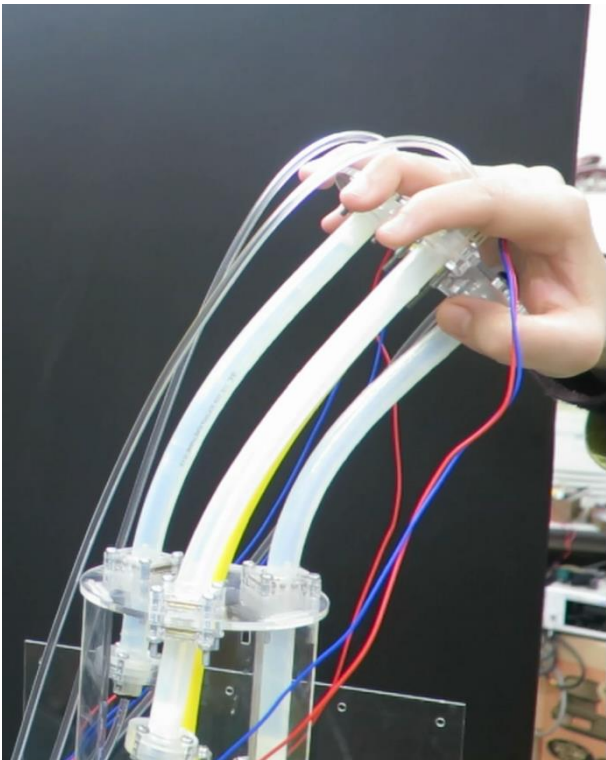


Fig. 1: Flexible pneumatic robot arm

## 2. Methodology

### 2.1 Flexible pneumatic cylinder and robot arm

Fig. 2 shows the construction of the flexible pneumatic cylinder. It consists of a flexible tube, two types of steel balls that have diameters of 9 mm and 3 mm, brass rollers and a slide stage. The flexible tube as a cylinder which allows air to pass through it is made of the soft polyurethane tube (SMC Co Ltd, TUS 1208). The 9 mm steel ball as a cylinder head is pinched by two pairs of brass rollers from both sides. This allows the ball to move freely when air enters into the cylinder.

The 3 mm steel balls are inserted between the slide stage and the flexible tube to hold the cylinder and brass rollers and at the same time to enable natural movement for the tube. When the pressure is applied from one end of the flexible tube, the 9 mm steel ball which is in the middle of the slide stage is

pushed and moved accordingly. At the same time, the steel ball pushes the brass rollers and then the slide stage moves while it deforms the tube. By using various center distance  $D$  and distance  $W$  between two pairs of rollers as a design parameter, the optimal combination between  $D$  and  $W$  so that the driving pressure of the pneumatic cylinder becomes minimum had been investigated by the experiment. The result shows that the best value for  $D$  is 14.4 mm and  $W$  is 10 mm (Akagi and Dohta, 2007). In this combination, the frictional force of the slide stage is small and the 9 mm steel ball does not get out from the slide stage.

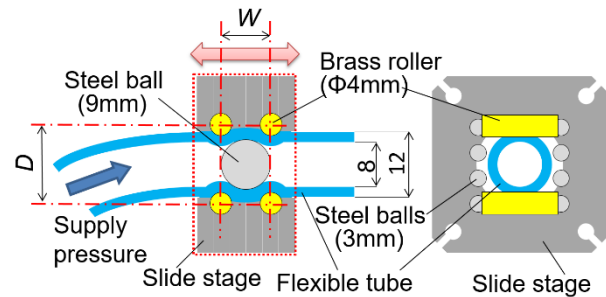


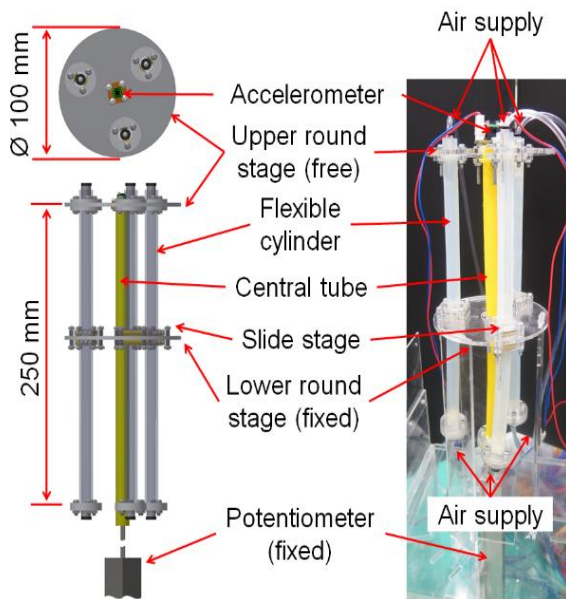
Fig. 2: Construction of the flexible pneumatic cylinder

Table 1 shows the properties of the flexible pneumatic cylinder that have been used for our pneumatic robot arm. Fig. 3 shows the construction of the flexible robot arm using flexible pneumatic cylinders (Aliff et al., 2012; Fujikawa et al., 2010). The robot arm consists of two round stages: an upper and a lower, three flexible pneumatic cylinders, a central tube, an accelerometer, a potentiometer and three slide stages. The potentiometer (Copal Electronics, stroke: 100 mm) is connected to the central tube as shown in Fig. 3 to measure the distance between two round stages. The size of the robot arm is  $\text{Ø}100 \text{ mm} \times 250 \text{ mm}$  and the mass is 380 g. The initial distance between the upper and lower stage is about 100 mm. Each flexible pneumatic cylinder is arranged so that the central angle of two adjacent slide stages becomes 120 degrees on the stage. An end of each flexible cylinder is fixed to the upper stage. The two quasi-servo valves (Zhao et al., 2010) which consist of four on/off valves (Koganei Co. Ltd., G010HE-1) are used to drive one flexible pneumatic cylinder. In order to control the three flexible cylinders, six control valves are needed. The maximum bending angle of the robot arm is 45 degrees and the total generated force of three cylinders is 45 N for the supply pressure of 500 kPa. In the flexible pneumatic cylinder as shown in Fig. 2, the tube is moved towards pressurized side when the slide stage is fixed. This driving method is used in this robot arm. The basic operating principle of the flexible robot arm is as follows. To make the arm extend or contract, pressure must be applied on one end of the cylinder only. To perform a bending motion to the right, for example, the right cylinder requires pressure from both ends to limit movement while the remaining two cylinders require pressure from

the top to enable movement (Aliff et al., 2014). The robot arm will bend by constricting one cylinder and extending the others. The upper round stage moves in the range of 0 to 180 mm with three cylinder tubes.

**2.2. Master slave control**

Fig. 4 shows the analytical model of robot arm. In this model, the shape of the flexible pneumatic cylinder between the lower stage and upper stage is assumed to always be a circular arc when the robot arm is bent. From the center of the robot, the bending angle from X axis is a bending direction angle  $\alpha$  while the bending angle  $\beta$  is defined as the angle between the normal vectors from the center of the upper surface of the Z axis of robot arm.



**Fig. 3:** Flexible pneumatic robot arm

**Table 1:** Properties of flexible pneumatic cylinder

Min. driving pressure	120kPa
Generated force	16N (input: 500kPa)
Max. moving speed	> 1m/s
Weight (stroke of 1m)	< 0.1kg
Min. radius of curvature	about 30mm
Max. working pressure	600kPa
Working temperature	From -20 to +60°C
Movement	Push-pull actions

The flexible pneumatic cylinder which is on the X axis is marked as cylinder 1 and the cylinders which are arranged in a counter clockwise direction are marked as cylinder 2 and cylinder 3.  $L_1, L_2,$  and  $L_3$  are the cylinder length (displacement) for cylinder 1, cylinder 2 and cylinder 3, respectively. From the geometric relationship as shown in Fig. 4, the following equations can be obtained (Eq. 1)

$$R = \frac{L}{\beta} \tag{1}$$

further, from Fig. 4,  $L_1, L_2,$  and  $L_3$  (length of the cylinder between the upper surface of the stage and lower stage) length of each cylinder are given by the following equations (Eqs. 2-4)

$$L_{1i} = (R_i - r \cdot \cos \alpha_i) \cdot \beta_i \tag{2}$$

$$L_{2i} = \left\{ R_i - r \cdot \cos \left( \frac{2\pi}{3} - \alpha_i \right) \right\} \cdot \beta_i \tag{3}$$

$$L_{3i} = \left\{ R_i - r \cdot \cos \left( \frac{4\pi}{3} - \alpha_i \right) \right\} \cdot \beta_i \tag{4}$$

where  $r$  is 33 mm that is the distance from the centre of the round stage to the centre of slide stage in the cylinder. Subscript  $i=m,s$  indicates for master arm (desired value) and the slave arm (present value), respectively. Subscript number (1, 2 and 3) indicates the location number of the cylinder. By using from the Eq. 1 to Eq. 4 and based on the displacement of the master and slave cylinder, the control system can be performed.

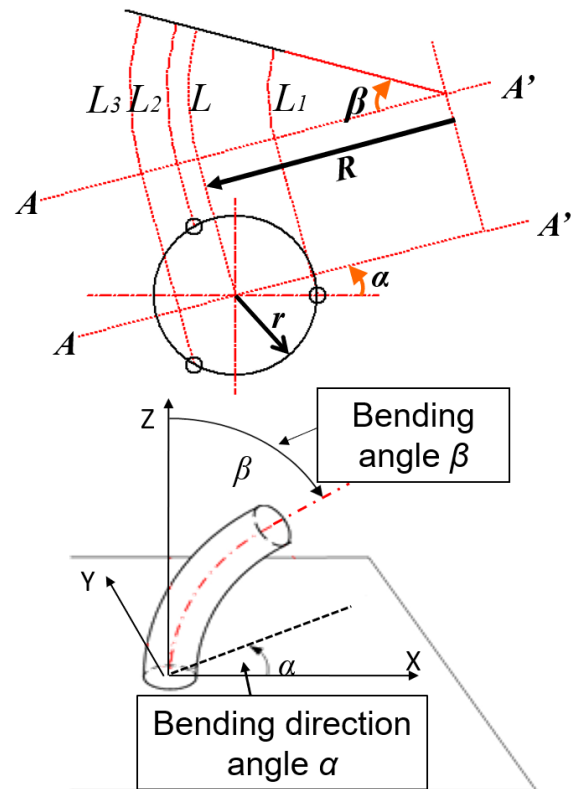


**Fig. 4:** Analytical model of robot arm

Fig. 5 shows the relationship between the bending angle and the output voltage from the accelerometer sensor. In this study, the bending direction angle  $\alpha$  and the bending angle  $\beta$  are measured by the accelerometer (Kionix KXR94-2050) which consists of a mass, a spring and a capacitance type displacement sensor. The acceleration can be calculated by the displacement of the mass. From Fig. 5, the following equations can be obtained (Eqs. 5 and 6).

$$\alpha = \cos^{-1} \frac{V_x}{\sqrt{V_x^2 + V_y^2}} \tag{5}$$

$$\beta = \cos^{-1} \left( \frac{V_z}{V_{zmax}} \right) \tag{6}$$

where  $V_x, V_y,$  and  $V_z$  are the output voltages from the accelerometer. The voltages  $V_x$  and  $V_y$  correspond to the angle from the horizontal plane and  $V_z$  corresponds to the angle from the vertical plane. The



$V_{zmax}$  means the difference of  $V_z$  between the values in horizontal and vertical planes.

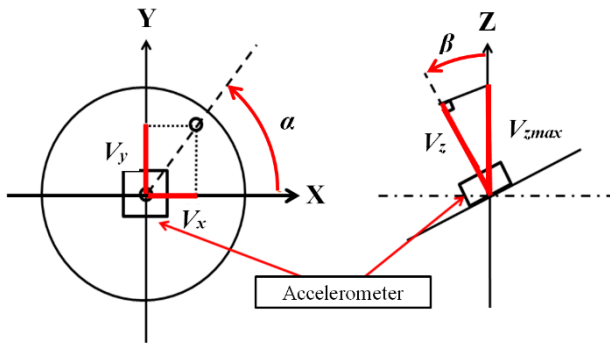


Fig. 5: The relationship between the bending angle and the output voltage from accelerometer sensor

By using from Eq. 1 to Eq. 6, we can calculate the length of cylinders for every bending state of the robot arm. In our previous study, we had confirmed that the calculated angle agreed well with the measured value (Fujikawa et al., 2010). The error between the calculated angles by Eq. 5 and Eq. 6 and the measured error angles were less than 1 degree.

**2.3. Master-slave control system and control procedure**

Fig. 6 and Fig. 7 show the view of the master-slave control system and its schematic diagram, respectively. It consists of a slave arm and a master arm. The slave arm consists of the tested robot arm, a potentiometer, an accelerometer sensor, a microcomputer (Renesas Co. Ltd., SH/7125) as the controller and six quasi-servo valves for driving the three flexible pneumatic cylinders.

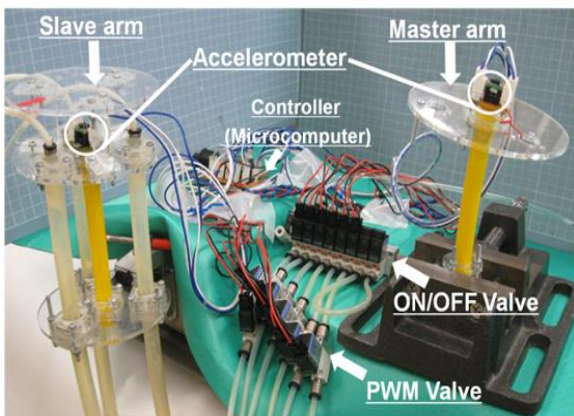


Fig. 6: The construction of master-slave control system

The master arm consists of a potentiometer and an accelerometer that is set atop of the upper round stage to give the reference attitude value. From Fig. 7, the microcomputer can get the output voltages of the accelerometer from the master and slave arm. The attitude of the upper round stage of the robot arm is detected with the accelerometer installed atop of the stage. The accelerometer can detect the bending angle of the upper stage by measuring the change of gravity for X, Y, and Z axes.

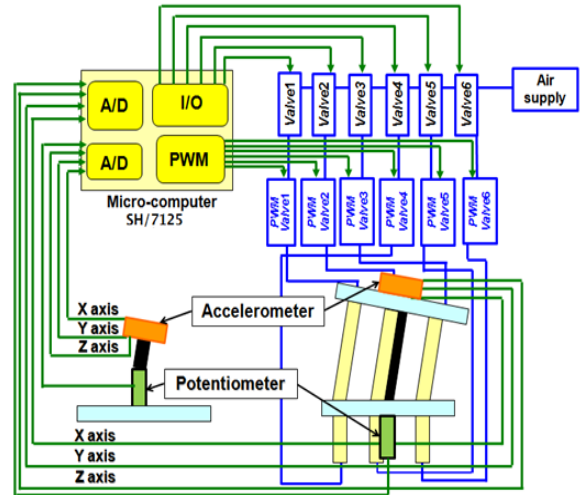


Fig. 7: Schematic diagram for control system

From these values, the bending direction angle  $\alpha$  and the bending angle  $\beta$  are calculated by using Eq. 5 and Eq. 6. The sampling period for control is 2.3 ms. Fig. 8 shows the block diagram of the master-slave control system. From Fig. 7 and Fig. 8, it is easily understood how the proposed master-slave control system works. The proposed control procedure is as follows:

1. First, the attitude of the master arm; the bending direction angle  $\alpha_m$ , the bending angle  $\beta_m$  and the distance  $L_m$  are detected by using the accelerometer and the potentiometer which are installed on it.
2. The distances on the master arm  $L_{1m}$ ,  $L_{2m}$  and  $L_{3m}$  are calculated by the microcomputer using the analytical model from Eq. 1 to Eq. 4.
3. Then, the attitude of the slave arm;  $\alpha_s$ ,  $\beta_s$  and  $L_s$  are detected by the accelerometer and the potentiometer of the slave arm. And the distances  $L_{1s}$ ,  $L_{2s}$  and  $L_{3s}$  are calculated by using the analytical model.
4. The errors between  $L_{jm}$  for the master arm and  $L_{js}$  ( $j=1, 2, 3$ ) for the slave arm are calculated with the microcomputer.
5. Finally, by using the quasi-servo valve (PWM control valve) and PID control scheme based on the calculated errors, the position of the cylinder can be controlled.

Microcomputer gets the output voltage from the bending angles and calculates the desired length and the present length of each flexible cylinder by using Eq. 1 to Eq. 4. The "length of the flexible cylinder" can be defined as the distance between the upper round stage and the lower stage. By using this method, each length of the flexible cylinder can be controlled. The variables output from microcomputer needs to be converted from digital signal into the analog signal in order to record it. So, we had developed the D/A converter and record the variables output voltage such as for bending direction angle  $\alpha$  and the displacement of the

cylinders  $L_1, L_2$  and  $L_3$  by using GRAPHTEC, GL200 recorder.

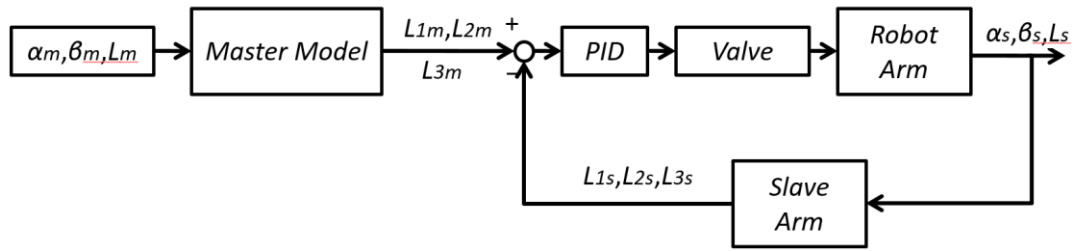


Fig. 8: Block diagram of master-slave control

3. Results and discussion

In order to confirm the effectiveness of the proposed model and identified system parameters, it is necessary to compare the calculated result of the analytical model for the overall robot arm with the experimental result. For the master-slave control method by using the tested quasi-servo valve, the following typical PID control scheme was embedded into the microcomputer (Eqs. 7 and 8)

$$u_i = \left| K_p e_i + K_i \int e_i dt + K_D \frac{de_i}{dt} \right| + 22.5 \quad (i = 1 \sim 3) \quad (7)$$

$$e_i = L_{im} - L_{is} \quad (i = 1 \sim 3) \quad (8)$$

where  $u_i$  [%] and  $e_i$  [m] mean the duty ratio for the PWM valve in the quasi-servo valve and the error of the cylinder displacement respectively. The value of 22.5 % is added to the control input to compensate the dead zone of a quasi-servo valve (Zhao et al., 2010). When the value in the absolute in Eq. 7

becomes negative, the switching valve in the quasi-servo valve switches to the exhaust from the supply. PID control parameters used in the experiment and simulation are listed in Table 2. These values were selected so that the control error became smaller and the movement of robot arm became smoother.

Table 2: PID control parameters

	$K_p$ [%/mm]	$K_i$ [%/(mm·s)]	$K_D$ [%·s/mm]
Master-slave control	0.87	2.5	0.0067

Fig. 9 shows the experimental result of the master-slave control. In these figures, the blue lines are the length values of the desired master cylinders and the red lines are the length values of the flexible slave cylinders. The frequency of the movement is about 0.2 Hz as can be found in Fig. 9.

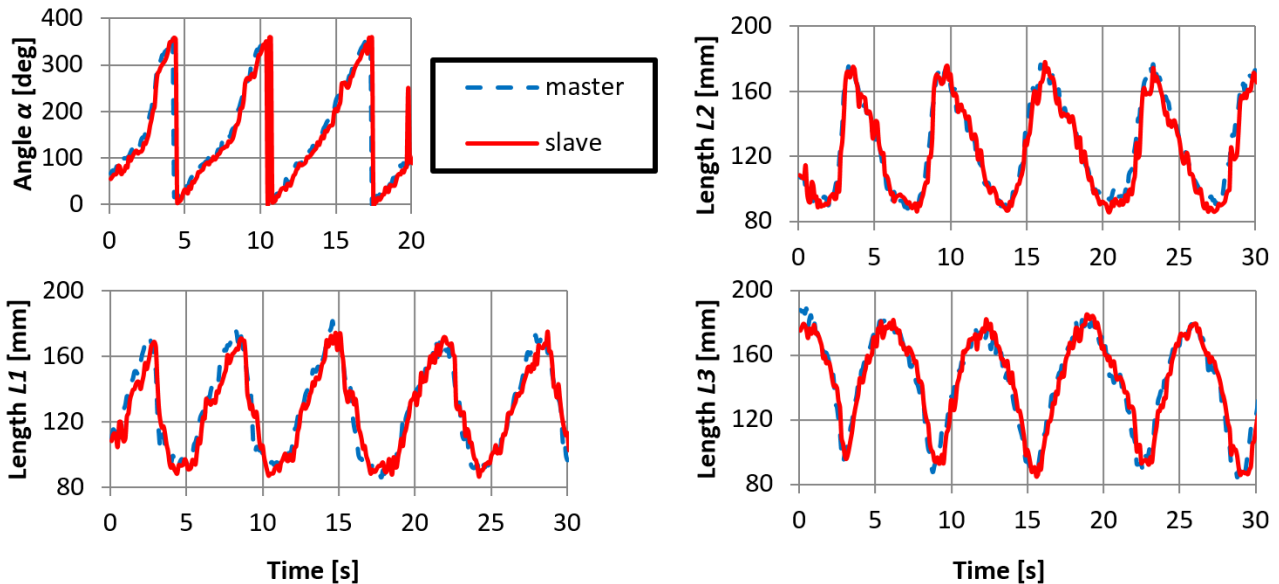


Fig. 9: Master-slave control result

During the experiment, the master arm is operated by a human hand to be bent, extended and contracted. While, the slave arm just follows the control movements from the master arm. From these figures, there are minor errors which the robot arm cannot trace the attitude of master arm. It can be seen that the length  $L_1, L_2$ , and  $L_3$  of slave arm has a small rapid-stepwise change. This minor error is caused by the large friction between the cylinders and the slide stages. However, from overall review

the slave arm can trace well the position of the master arm. Thus, we can confirm that the effectiveness of the control method can be achieved by using the proposed analytical model and the tested quasi-servo valve.

Fig. 10 shows the calculated result of the master-slave control for the bending direction angle  $\alpha$  and each cylinder length  $L_1, L_2$  and  $L_3$ . In these figures, the black lines are the desired target values which are calculated by using previously proposed

equations, based on the accelerometer's output voltages of the master arm and the red lines are the calculated results using the proposed overall analytical model of the robot arm (Aliff et al, 2014). In both experiment and simulation, the values of  $\beta$  and  $L$  are kept constant:  $\beta = 73$  deg. and  $L = 0.131$  m. In the calculation, Matlab Simulink with Runge-Kutta method was used. In the same way as the

experiment, the sampling period of 2.3 ms of the embedded controller with 10 bit A/D converter and the PWM period of 10 ms for the quasi-servo valve were used. From the comparison between the calculated values and the experimental values, it can be seen that the calculated results agree well with the experimental results.

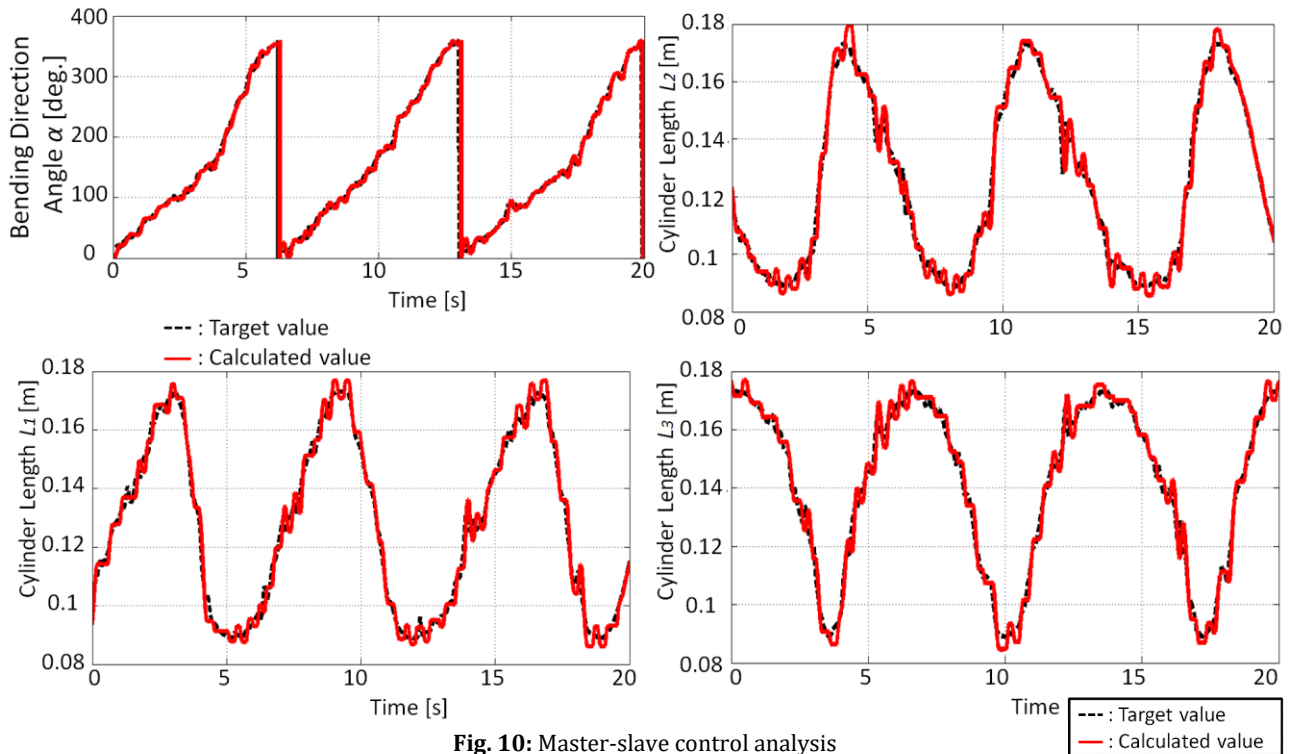


Fig. 10: Master-slave control analysis

#### 4. Conclusion

This study focusing on the control and analysis of the simple-structured robot arm using flexible pneumatic cylinder can be summarized as follows:

- The compact and light-weight control system of the flexible robot arm for the master-slave control was proposed and tested. The system consists of the microcomputer, compact and inexpensive quasi-servo valves, accelerometers and the tested robot arm.
- The simulation of the master-slave control using the proposed method was executed by using the previously proposed analytical model of whole robot arm system. As a result of comparison, the calculated results agreed with the experimental results. The results show that the proposed analytical model can predict the behavior of the robot arm and the master-slave control.

#### References

Akagi T and Dohta S (2007). Development of a rodless type flexible pneumatic cylinder and its application. Nippon Kikai Gakkai Ronbunshu C Hen (Transactions of the Japan Society of Mechanical Engineers Part C)(Japan), 19(7): 2108-2114.

Aliff M, Dohta S, Akagi T, and Li H (2012). Development of a simple-structured pneumatic robot arm and its control using

low-cost embedded controller. *Procedia Engineering*, 41: 134-142.

Aliff M, Dohta S, and Akagi T (2014). Control and analysis of robot arm using flexible pneumatic cylinder. *Mechanical Engineering Journal*, 1(5): 1-13.

Dohta S, Akagi T, Aliff M, and Ando A (2013). Development and control of simple-structured flexible mechanisms using flexible pneumatic cylinders. In the IEEE/ASME International Conference on Advanced Intelligent Mechatronics, IEEE, Wollongong, NSW, Australia: 888-893. <https://doi.org/10.1109/AIM.2013.6584206>

Fujikawa T, Dohta S, and Akagi T (2010). Development and attitude control of flexible robot arm with simple structure using flexible pneumatic cylinders. In the 4<sup>th</sup> Asia International Conference on Mechatronics: 136-141. [https://doi.org/10.3850/978-981-08-7723-1\\_P169](https://doi.org/10.3850/978-981-08-7723-1_P169)

Ishii M, Yamamoto K, and Hyodo K (2005). Stand-alone wearable power assist suit development and availability. *Journal of Robotics and Mechatronics*, 17(5): 575-583.

Kobayashi H, Ishida Y, and Suzuki H (2004). Realization of all motion for the upper limb by a muscle suit. In the 13<sup>th</sup> IEEE International Workshop on Robot and Human Interactive Communication, IEEE, Kurashiki, Okayama, Japan: 631-636. <https://doi.org/10.1109/ROMAN.2004.1374835>

Lum PS, Burgar CG, and Shor PC (2004). Evidence for improved muscle activation patterns after retraining of reaching movements with the MIME robotic system in subjects with post-stroke hemiparesis. *IEEE Transactions on Neural Systems and Rehabilitation Engineering*, 12(2): 186-194.

- Noritsugu T, Takaiwa M, and Sasaki D (2009). Development of power assist wear using pneumatic rubber artificial muscles. *Journal of Robotics and Mechatronics*, 21(5): 607-613.
- Piquion J, Nayar A, Ghazaryan A, Papanna R, Klimek W, and Laroia R (2009). Robot-assisted gynecological surgery in a community setting. *Journal of Robotic Surgery*, 3(2): 61-64.
- Reinkensmeyer DJ, Dewald JPA, and Rymer WZ (1999). Guidance-based quantification of arm impairment following brain injury: A pilot study. *IEEE Transactions on Rehabilitation Engineering*, 7(1): 1-11.
- Yassin IM, Zabidi A, Ali MSAM, Tahir NM, Abidin HZ, and Rizman ZI (2016). Binary particle swarm optimization structure selection of nonlinear autoregressive moving average with exogenous inputs (NARMAX) model of a flexible robot arm. *International Journal on Advanced Science, Engineering and Information Technology*, 6(5): 630-637.
- Zhao F, Dohta S, and Akagi T (2010). Development and analysis of small-sized quasi-servo valve for flexible bending actuator. *Transactions of Japan Society of Mechanical Engineers*, 76(772): 3665-3671.
- Zheng H, Davies R, Zhou H, Hammerton J, Mawson SJ, Ware PM, and Black ND (2006). SMART project: Application of emerging information and communication technology to home-based rehabilitation for stroke patients. *International Journal of Disability and Human Development*, 5(3): 271-276.